



In-plane elastic properties of hierarchical nano-honeycombs: The role of the surface effect

Qiang Chen^a, Nicola M. Pugno^{b,c,d,*}

^a School of Biological Science and Medical Engineering, Southeast University, 210096 Nanjing, P.R. China

^b Laboratory of Bio-inspired Nanomechanics, Department of Structural, Geotechnical and Building Engineering, Politecnico di Torino, Corso Duca degli Abruzzi, 24, 10129 Torino, Italy

^c National Institute of Nuclear Physics, National Laboratories of Frascati, Via E. Fermi 40, 00044 Frascati, Italy

^d National Institute of Metrological Research, Strada delle Cacce 91, I-10135 Torino, Italy

ARTICLE INFO

Article history:

Received 17 January 2012

Accepted 11 June 2012

Available online 19 June 2012

Keywords:

Hierarchical
Nano-honeycomb
Elasticity
Buckling
Strength

ABSTRACT

In this paper, we analytically calculate the in-plane elastic properties (linear-elasticity and elastic buckling) of a new class of bio-inspired nano-honeycomb materials possessing a hierarchical architecture. Incorporating the surface effect, modifications to the classical results for macroscopic and nonhierarchical honeycombs are proposed, and the results are compared with those in the literature. A parametrical analysis reveals the influences of two key geometrical parameters on the overall elastic properties. We discuss the relevant mechanical properties, e.g. stiffness efficiency (stiffness-to-density ratio) and strength efficiency (strength-to-density ratio), which are indices reflecting the mechanical efficiency of materials, and discover that the structural strength can be optimized. The developed theory allows us to design a new class of nano materials with tailored mechanical properties at each hierarchical level and could be useful for many applications.

© 2012 Published by Elsevier Masson SAS.

1. Introduction

Honeycomb-like structure can be often found in Nature, for instance, the armadillo shell (Rhee et al., 2011), the beak of Tucan birds (Seki et al., 2005), and the widely studied lobster claws of lobsters (Raabe et al., 2005): the structure is low-weight but strong and tough, that is to say, it is more efficient (Karam and Gibson, 1994). So far, it is well accepted that the structure of the natural materials is an optimized result by ambient environment in the evolutionary process (e.g. the armadillo shell can protect internal organs from being attacked by predators). Thus, nature seems to grant us a best solution to design more efficient materials. Therefore, inspired by nature, honeycomb materials have been extensively investigated for structural, mechanical and material design. For example, in the field of material science, they are used as a core material in sandwich structures for energy absorption (Wang, 2009; Wang et al., 2009); also, honeycomb scaffolds with mechanical stability, biocompatibility and biodegradability are used for tissue regeneration (George et al., 2008). With such extensive applications, from the mechanical point of view, it is

important for materials scientists and engineers to characterize and model the in-plane and out-of-plane mechanical behaviors (Gibson et al., 1982; Warren and Kraynik, 1987; Zhang and Ashby, 1992; Papka and Kyriakides, 1994) of honeycomb structures. For its constitutive behavior, the stress–strain curves (Papka and Kyriakides, 1994; Gibson and Ashby, 1997) are typically described by three regimes (the linear elastic, pseudo plastic plateau and pseudo hyper-elastic densification regions). Gibson and Ashby (1997) summarized most of the works on the structural and mechanical properties for 2D and 3D cellular solids, and systematically investigated the structure–solid mechanics. In recent years, a variety of topological honeycombs is being studied for multifunctional applications (Wadley, 2006), e.g. the thermal conductivity properties of a rectangular-hexagonal honeycomb structure (Bezazi et al., 2008). Even though many studies in this field provide some methods to design new porous materials, and enrich the existing ones, there is a lack of detailed investigations on natural honeycombs. So, in order to mimic the natural honeycomb, Zhang et al. (2010) revealed the sophisticated and hierarchical structure of honeybee combs, and showed that the cell wall of the natural honeycomb is a multi-layered structure, which is continuously constructed by adding wax layers reinforced by silk as time increases; the structure is strengthened and avoids the fragility, and thus provides a mechanically safe place for storing honey and brooding.

* Corresponding author. Department of Structural, Geotechnical and Building Engineering, Politecnico di Torino, Corso Duca degli Abruzzi, 24, 10129 Torino, Italy. Tel.: +39 (0)115644902.

E-mail address: nicola.pugno@polito.it (N.M. Pugno).

On the other hand, as nanoscience and nanotechnology develop, the material design also expands towards the nano-scale. If structures are nano-sized, the surface effect should be taken into account, due to their high surface-to-volume ratio. Regarding the surface effect, extensive works (Wang and Feng, 2009; Shankar and King, 2007; Wong et al., 1997; Chen and Pugno, 2012a) studied its influence on the linear elastic behaviors of nano-wires, since they hold a promise for nano-device applications, e.g. sensors and actuators. These works emphasized the vital role of the surface effect in determining the mechanics of nano-systems. Duan et al. (2006, 2009) investigated the elastic constants of nanoporous materials with unidirectional cylindrical nanochannels by considering the surface effect, and the results demonstrated that a nanoporous material could be stiffer or softer than its bulk counterpart. And more, Duan et al. (2009) reviewed the elastic theory for nano-scale systems, especially for the nanoscale inhomogeneities, discussing different classical theories, e.g. Eshelby Formalism, and Levin's formulas. These works are very useful for studying the fundamental mechanical and physical properties of heterogeneous nanosystems.

In this paper, we construct a hierarchical nano-honeycomb structure (Fig. 1), using a classical iterative approach (Lakes, 1993; Pugno, 2006; Pugno et al., 2008; Chen and Pugno, 2012b,c), and study its in-plane elastic properties. Starting from an orthotropic constituent material and considering the influence of the surface effect, we derived the effective longitudinal Young's modulus and buckling strength at the first level; then, the results of the n -level structure ($n \geq 2$) are obtained thanks to the iterative method. Finally, a comparison between different theories and parametric analyses reveal the influences of the geometrical parameters on the overall elastic behaviors.

2. Surface effect

Due to the existence of surfaces in a solid, there is always a competition between bulk and surface. In particular, when the size of the solid comes down into dimensions smaller than 10 nm, surface/interface effect becomes an important characteristic in nanostructures, and determines their mechanical properties. A classical expression for the surface stress is derived based on the surface/interface energy (Cammarata, 1994), and it is composed by two parts, i.e. surface free energy and surface free energy gradient with respect to the surface strain: $f_{ij} = \gamma\delta_{ij} + \partial\gamma/\partial\varepsilon_{ij}$, where, f_{ij} and ε_{ij} are the surface stress and strain tensors, respectively, γ is the surface free energy, δ_{ij} is the Kronecker delta.

For the elastic theory, according to Gurtin and Murdoch (1975), the surface stress τ is usually expressed as the summation of the

surface residual stress and surface elasticity (i.e. the two parts corresponding to the two terms on the right-handed side of the f_{ij} expression, respectively): $\tau = \tau^0 + S^i\varepsilon^i$, where, τ^0 is the surface residual stress, S^i is the surface stiffness tensor, ε^i is the surface elastic strain tensor. Here, we only consider the influence of the surface elasticity (one-dimension), i.e. the second term on the right-handed side of the τ expression.

3. Elastic constants of hierarchical nano-honeycombs

3.1. Deflection of an orthotropic beam with surface elasticity

The linear-elastic deformation mechanism of honeycombs is mainly due to the bending of cell walls, and the standard beam theory is employed here to investigate their elastic constants. (Fig. 2); in particular, if the beam is nano-sized, the modification induced by the surface effect should be taken into account, and the maximum displacement of the Euler beam is expressed (Tolf, 1985; Roark and Young, 1975; Gibson and Ashby, 1997; Wang and Feng, 2009) as:

$$\delta_{\max} = \frac{F l^3}{12(E_1 I)^{\text{eq}}} \cos^2 \theta \quad \text{if } \tau^0 = 0 \quad (1)$$

with

$$(E_1 I)^{\text{eq}} = \frac{1}{12} E_1 b t^3 + \frac{1}{2} E_s b t^2 + \frac{1}{6} E_s t^3 \quad (2)$$

where, δ_{\max} is the vertical displacement of the guided end of the orthotropic beam, F is the concentrated force acting on the guided end, l is the beam length, θ is the inclined angle between beam and horizontal line; $(E_1 I)^{\text{eq}}$ is the equivalent flexural rigidity considering the surface effect; b , t are width and thickness of the beam, respectively; E_s , depending on the crystal orientation (Shenoy, 2005), is the surface Young's modulus, which has the physical dimensions of a surface tension.

3.1.1. One-level structure

First, we consider a one-level nano-honeycomb made by an orthotropic material (level 0) and introduce a local coordinate system $1^{(0)}2^{(0)}$ related to the global coordinate system $1^{(1)}2^{(1)}$. As shown in Fig. 3, the structure has two perpendicular mirror planes, i.e. the one-level structure remains orthotropic. The deformation is caused by the bending of beams ①, ② and the compression of beam ③ (Fig. 3(b)) which is the beam parallel to the loading direction, but

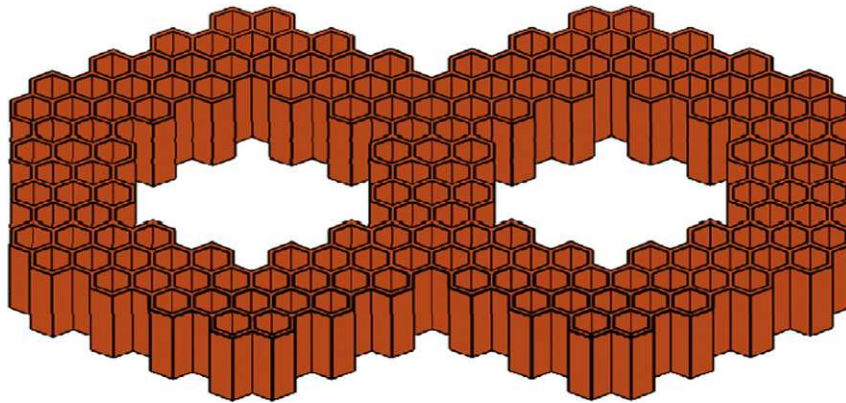


Fig. 1. Two-level nano-honeycombs.

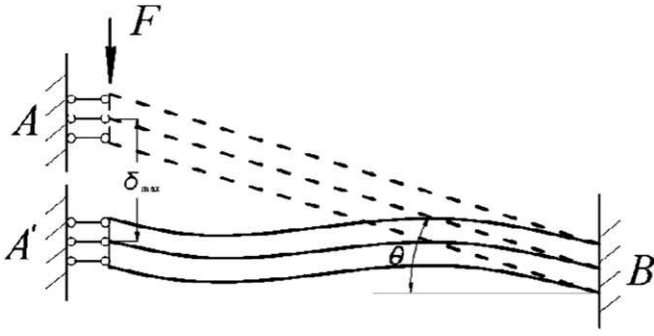


Fig. 2. An inclined orthotropic beam with one end guided and the other fixed.

the compressive deformation is neglected with respect to the bending deflection. Thus, basing on equations (1) and (2) and employing the classical approach (Gibson and Ashby, 1997), we find the elastic constants of the one-level nano-honeycomb:

$$\frac{E_1^{(1)}}{E_1^{(0)}} = \lambda_s^{(1)} f_1^{(1)} f_4^{(1)} \left(\frac{\rho^{(1)}}{\rho^{(0)}} \right)^3 \quad (3)$$

$$\frac{E_2^{(1)}}{E_1^{(0)}} = \frac{f_2^{(1)}}{f_1^{(1)}} \cdot \frac{E_1^{(1)}}{E_1^{(0)}} \quad (4)$$

$$\frac{G_{12}^{(1)}}{E_1^{(0)}} = \frac{f_3^{(1)}}{f_1^{(1)}} \cdot \frac{E_1^{(1)}}{E_1^{(0)}}$$

$$\mu_{12}^{(1)} = \left(\frac{f_1^{(1)}}{f_2^{(1)}} \right)^{0.5} = \frac{1}{\mu_{21}^{(1)}} \quad (5)$$

with

$$\lambda_s^{(1)} = 1 + 2 \frac{E_s^{(0)}}{E_1^{(0)} t^{(1)}} \left(3 + \frac{t^{(1)}}{b} \right) \quad (6)$$

$$\begin{aligned} f_1^{(1)} &= \frac{(h^{(1)}/l^{(1)} + \sin \theta^{(1)})}{\cos^3 \theta^{(1)}} \\ f_2^{(1)} &= \frac{\cos \theta^{(1)}}{(h^{(1)}/l^{(1)} + \sin \theta^{(1)}) \sin^2 \theta^{(1)}} \\ f_3^{(1)} &= \frac{(h^{(1)}/l^{(1)} + \sin \theta^{(1)})}{(h^{(1)}/l^{(1)})^2 (1 + 2h^{(1)}/l^{(1)}) \cos \theta^{(1)}} \\ f_4^{(1)} &= \left(\frac{2 \cos \theta^{(1)} (h^{(1)}/l^{(1)} + \sin \theta^{(1)})}{(h^{(1)}/l^{(1)} + 2)} \right)^3 \end{aligned} \quad (7)$$

where $E_1^{(0)}$ and $E_s^{(0)}$ are the bulk and surface Young's moduli in the principal direction 1⁽⁰⁾ (level 0), respectively; b and $t^{(1)}$ are width and thickness of cross-sections of cell walls, respectively; $l^{(1)}$ and $h^{(1)}$ are lengths of beams ① and ③, respectively; $\theta^{(1)}$ is the included angle made by beam ① and horizontal line (Fig. 3).

From equations (3)–(7), we note that compared with the Young's moduli and shear modulus derived by Gibson and Ashby (1997), here, the Young's moduli and shear modulus of the one-level structure are modified by a factor $\lambda_s^{(1)}$. If $t_1^{(1)}/b \ll 1$ (plate), equation (6) can be expressed as:

$$\lambda_s^{(1)} = 1 + 6 \frac{E_s^{(0)}}{E_1^{(0)} t^{(1)}} \quad (8)$$

Expression (8) coincides with the result from Miller and Shenoy (2000), and it obeys the scaling law $\lambda_s^{(1)} = 1 + \alpha l_{in}/t^{(1)}$ (Wang et al., 2006) with $l_{in} = E_s^{(0)}/E_1^{(0)}$ and $\alpha = 6.0$. Note that: l_{in} represents an intrinsic material length, under which surface effect plays an important role; α is a dimensionless constant, which depends on the structural geometry and loading methods. Besides, we can see that the surface effect at level 0 makes the structure stiffer if $E_s^{(0)} > 0$; otherwise, it makes the structure softer.

Moreover, the geometry of Fig. 3 provides the relative density:

$$\frac{\rho^{(1)}}{\rho^{(0)}} = \frac{(h^{(1)}/l^{(1)} + 2)}{2 \cos \theta^{(1)} (h^{(1)}/l^{(1)} + \sin \theta^{(1)})} \frac{t^{(1)}}{l^{(1)}} \quad (9)$$

where, $\rho^{(1)}$ and $\rho^{(0)}$ are densities of the one-level structure and its constituent material, respectively.

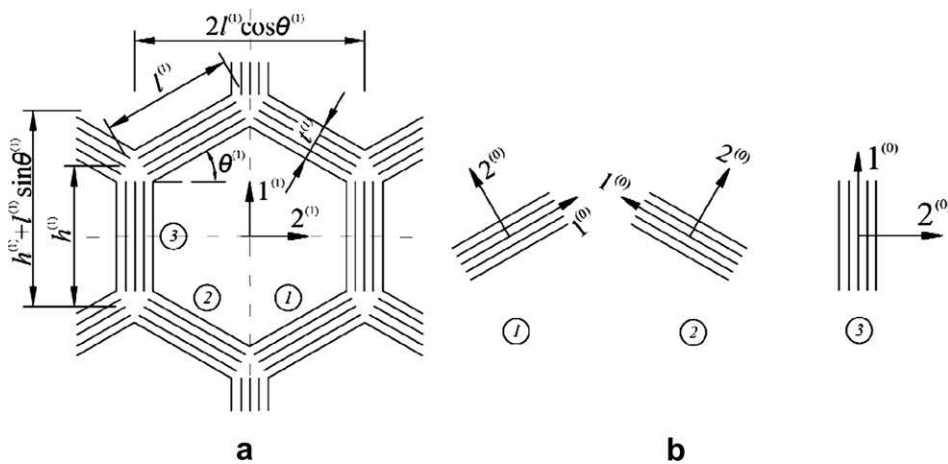


Fig. 3. Schematic of the first-level nano-honeycomb. (a) Unit cell; (b) Three pairs of cell walls.

3.1.2. *n*-Level structure

Fig. 4 describes an *n*-level nano-honeycomb. Compared with the one-level structure, the cell-wall dimensions at the second or above levels are very large, so the surface effect could be neglected, i.e. $E_s^{(i)} = 0$ ($i \geq 2$). However, in order to extend the theory to the general case, we still consider the surface effect at each level, then, iterating equation (3) we find:

$$\frac{E_1^{(n)}}{E_1^{(0)}} = \prod_{i=1}^n \lambda_s^{(i)} f_1^{(i)} f_4^{(i)} \cdot \left(\frac{\rho^{(n)}}{\rho^{(0)}}\right)^3 \quad (10)$$

$$\frac{E_2^{(n)}}{E_1^{(0)}} = \frac{f_2^{(n)}}{f_1^{(n)}} \cdot \frac{E_1^{(n)}}{E_1^{(0)}} \quad (11)$$

$$\frac{G_{12}^{(n)}}{E_1^{(0)}} = \frac{f_3^{(n)}}{f_1^{(n)}} \cdot \frac{E_1^{(n)}}{E_1^{(0)}}$$

$$\mu_{12}^{(n)} = \left(\frac{f_1^{(n)}}{f_2^{(n)}}\right)^{0.5} = \frac{1}{\mu_{21}^{(n)}} \quad (12)$$

where, $f_1^{(n)}$, $f_2^{(n)}$, $f_3^{(n)}$ and $f_4^{(n)}$ can be obtained by replacing the superscript (1) with (*n*) in equation (7). Note that, the reciprocal theorem holds i.e., $E_1^{(n)} \mu_{21}^{(n)} = E_2^{(n)} \mu_{12}^{(n)}$. Equations (10)–(12) show that the transverse Young’s modulus and shear modulus can be derived from the longitudinal Young’s modulus, and the two Poisson’s ratios are only related to the geometry of the *n*-level structure. Therefore, in essential, there are only two independent elastic constants, i.e. the longitudinal Young’s modulus and one of the Poisson’s ratios.

3.2. Stiffness efficiency

Structural efficiency is basing on the minimum-weight analysis, and it is used to optimize structural design and thus, reduce cost. By considering the maximum stress and maximum strain, Budiansky (1999) investigated several types of compressive structures which are hollow tubes with/without filling foam. Wegst and Ashby (2004) summarized the mechanical efficiency of natural ceramics,

natural polymers, natural elastomers, natural cellular materials under tensile and flexural loads and plotted the so-called “Ashby maps” according to different material indices. Here, according to Ashby (2010), we study the stiffness-to-density ratio for the honeycomb structure under the uniaxially loading condition, which is evaluated by $P_{s1} = E/\rho$. For the hierarchical honeycomb structures, $E_1^{(n)}/\rho^{(n)}$ can be derived from equations (9–11) as:

$$\frac{E_1^{(n)}}{\rho^{(n)}} = \frac{E_1^{(0)}}{\rho^{(0)}} \prod_{i=1}^n \lambda_s^{(i)} f_1^{(i)} f_4^{(i)} \cdot \left(\frac{\rho^{(n)}}{\rho^{(0)}}\right)^2 \quad (13)$$

$$\frac{E_2^{(n)}}{\rho^{(n)}} = \frac{f_2^{(n)}}{f_1^{(n)}} \cdot \frac{E_1^{(n)}}{\rho^{(n)}} \quad (14)$$

$$\frac{G_{12}^{(n)}}{\rho^{(n)}} = \frac{f_3^{(n)}}{f_1^{(n)}} \cdot \frac{E_1^{(n)}}{\rho^{(n)}}$$

4. Elastic buckling of hierarchical honeycomb materials

Different from the linear-elastic deformation of honeycombs, progressive buckling deformation of cell walls dominates the main energy-absorbing mechanism. Therefore, it is significant to study the buckling behavior of the hierarchical honeycomb in the design of energy-absorbing materials. Regarding the buckling behavior of the conventional honeycomb, Chen and Pugno (2012a) studied the competition between the buckling of the beam ① (or ②) and beam ③, and they demonstrated that the buckling of the beam ③ prevails and there is a possibility for the buckling occurrence of beam ① (or ②) at extreme conditions (e.g. the inclination angle approaches 90° and the thickness-to-length ratio of the beam ① (or ②) approaches zero). Therefore, we only consider the buckling of the beam ③ in the following discussion.

4.1. Buckling load of the orthotropic beam with surface effect

Euler buckling equation is a simple but efficient way to describe the buckling behavior for an isotropic beam or column. For an

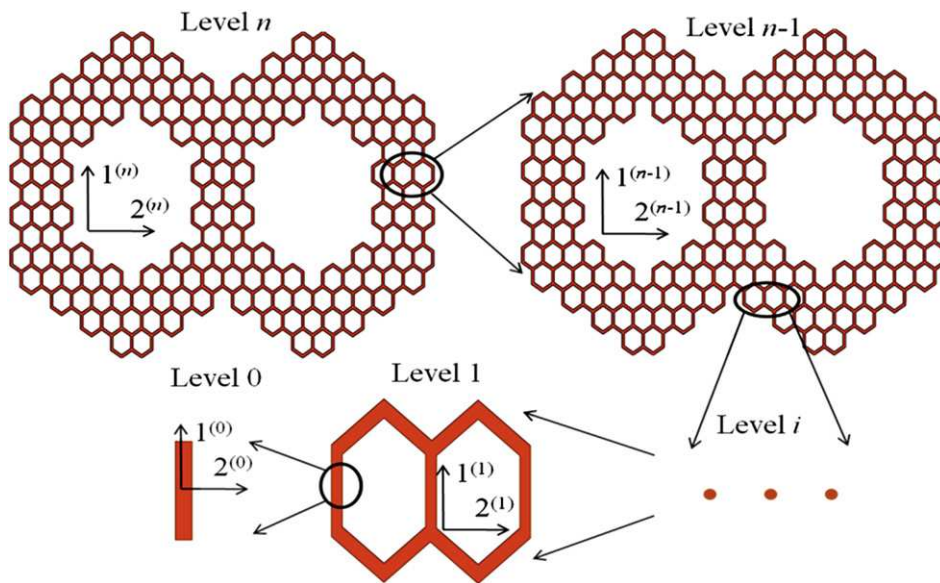


Fig. 4. Top view of the schematic of the *n*-level nano-honeycomb.

orthotropic nano-column, due to the standard beam theory (i.e. Euler beam theory) and the surface effect, the buckling load F_{cr} is obtained (Tolf, 1985; Timoshenko and Gere, 1961):

$$F_{cr} = \frac{n^2 \pi^2 (E_1 I)^{eq}}{l^2} \quad \frac{1}{2} \leq n \leq 2 \quad (15)$$

where, n is a numerical factor depending on the boundary conditions. Equation (15) is the classical Euler buckling formula with surface effect, in which the Young's modulus of the isotropic material is substituted by the longitudinal one of the orthotropic beam.

4.1.1. One-level structure

For the one-level structure (Fig. 3), when the external stress s acts on the structure (Fig. 1), the equivalent concentrated force applied on beam $\textcircled{3}$ is:

$$F^{(1)} = 2sb^{(1)}l^{(1)}\cos \theta^{(1)} \quad (16)$$

Then, if the beam buckles, the force F should reach the critical load F_{cr} . Substituting equation (16) into equation (15), we find:

$$\frac{s_{cr}^{(1)}}{E_1^{(0)}} = \lambda_s^{(1)} \frac{(\pi n^{(1)})^2}{24} \left(\frac{t^{(1)}}{l^{(1)}}\right)^3 \left(\frac{l^{(1)}}{h^{(1)}}\right)^2 \frac{1}{\cos \theta^{(1)}} \quad (17)$$

Here, we define a new function with respect to $h^{(1)}/l^{(1)}$ and $\theta^{(1)}$:

$$f_5^{(1)} = \frac{(\pi n^{(1)})^2}{24} \left(\frac{l^{(1)}}{h^{(1)}}\right)^2 \frac{1}{\cos \theta^{(1)}} \quad (18)$$

where, $n^{(1)}$ is related to $h^{(1)}/l^{(1)}$ and equation (17) is concisely written as:

$$\frac{s_{cr}^{(1)}}{E_1^{(0)}} = \lambda_s^{(1)} f_4^{(1)} f_5^{(1)} \left(\frac{\rho^{(1)}}{\rho^{(0)}}\right)^3 \quad (19)$$

4.1.2. Two-level structure

For the two-level structure, we have two objects in the analysis, the vertical beams at the first and the second level. On one hand, for the second level, the equivalent concentrated force acting on the beam is:

$$F^{(2)} = 2sb^{(2)}l^{(2)}\cos \theta^{(2)} \quad (20)$$

According to equation (20), we find the buckling stress for the beam:

$$\frac{s^{(2)}}{E_1^{(1)}} = \lambda_s^{(2)} f_4^{(2)} f_5^{(2)} \left(\frac{\rho^{(2)}}{\rho^{(1)}}\right)^3 \quad (21)$$

$E_1^{(1)}$ is calculated by equation (3), finally, equation (21) is rewritten as:

$$\frac{s^{(2)}}{E_1^{(0)}} = \left(\lambda_s^{(1)} \lambda_s^{(2)}\right) \left(f_1^{(1)} f_4^{(1)}\right) \left(f_4^{(2)} f_5^{(2)}\right) \left(\frac{\rho^{(2)}}{\rho^{(0)}}\right)^3 \quad (22)$$

On the other hand, based on load transfer and the equivalent concentrated force acting on the beam at the second level, the equivalent concentrated force acting on the beam at the first level can be calculated, which is expressed as:

$$F^{(1)} = 2 \left(2s \frac{l^{(2)}}{t^{(2)}} \cos \theta^{(2)}\right) b^{(1)} l^{(1)} \cos \theta^{(1)} \quad (23)$$

then, substituting the force into the buckling equation (15), the buckling stress is immediately obtained as:

$$\frac{s^{(1)}}{E_1^{(0)}} = \lambda_s^{(1)} f_6^{(2)} \left(f_4^{(1)} f_5^{(1)}\right) \left(\frac{\rho^{(1)}}{\rho^{(0)}}\right)^2 \left(\frac{\rho^{(2)}}{\rho^{(0)}}\right) \quad (24)$$

with

$$f_6^{(2)} = \frac{(h^{(2)}/l^{(2)} + \sin \theta^{(2)})}{(h^{(2)}/l^{(2)} + 2)} \quad (25)$$

For the buckling stress of the two-level structure, it is derived as:

$$s_{cr}^{(2)} = \min(s^{(2)}, s^{(1)}) \quad (26)$$

4.1.3. n-Level structure

Like the analysis of the two-level structure, finding the concentrated force acting on the beam at level i and substituting the force into buckling equation (15), the dimensionless buckling stress at each level is obtained as:

$$\frac{s^{(i)}}{E_1^{(0)}} = \prod_{j=i+1}^n f_6^{(j)} \cdot \prod_{k=1}^{i-1} \left(\lambda_s^{(k)} f_1^{(k)} f_4^{(k)}\right) \cdot \left(f_4^{(i)} f_5^{(i)}\right) \left(\frac{\rho^{(i)}}{\rho^{(0)}}\right)^2 \left(\frac{\rho^{(n)}}{\rho^{(0)}}\right) \quad (27)$$

so, the buckling load of the n -level structure is obtained as:

$$s_{cr}^{(n)} = \min(s^{(i)}) \quad (28)$$

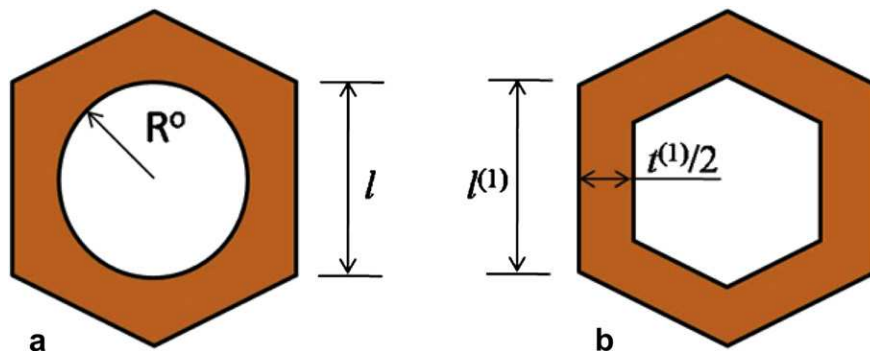


Fig. 5. (a) Unit cell of the honeycomb structure with cylindrical nano-channel; (b) Unit cell of the honeycomb structure with hexagonal nano-channel.

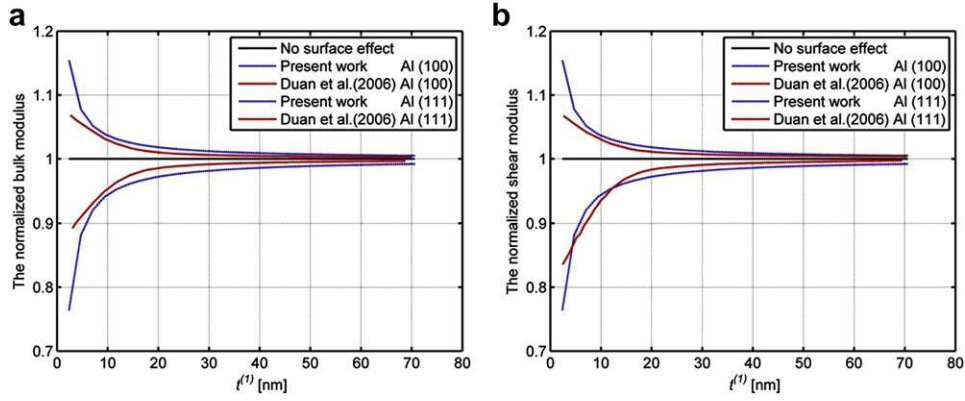


Fig. 6. (a) The normalized bulk modulus vs beam size; (b) The normalized Young's modulus vs beam size.

4.2. Strength efficiency

Like stiffness efficiency, the strength efficiency of the hierarchical structure is here deduced. And a for uniaxial loading structure, it is evaluated as $P_{s2} = s/\rho$. From equation (27), the evaluating criterion, i.e. buckling stress to density, is expressed as:

$$\frac{s^{(i)}}{\rho^{(n)}} = \prod_{j=i+1}^n f_6^{(j)} \cdot \prod_{k=1}^{i-1} (\lambda_s^{(k)} f_1^{(k)} f_4^{(k)}) \cdot (f_4^{(i)} f_5^{(i)}) \left(\frac{\rho^{(i)}}{\rho^{(0)}} \right)^2 \left(\frac{E_1^{(0)}}{\rho^{(0)}} \right) \quad (29)$$

thus, the buckling strength to density is finally obtained as:

$$\frac{s_{cr}^{(n)}}{\rho^{(n)}} = \min(s^{(i)}) \quad (30)$$

5. Comparison between different methods

In this section, we compare our predictions on the one-level structure ($\theta^{(1)} = 30^\circ$ and $h^{(1)}/l^{(1)} = 1$) with other results presented in the literature (Duan et al., 2006, 2009). In the literature, the unit cell of the nano-structure is honeycomb with unidirectional cylindrical nano-channels, thus different from our unidirectional hexagonal nano-channel (Fig. 5); the authors considered the cases with porosity 0.2 and pore diameter from 1 nm to 30 nm. Here, with the condition $l = l^{(1)}$, we compares the different geometries imposing the same pore area fractions.

Then, according to a porosity 0.2 and fixed geometry, see Fig. 5a, we find the relationship between the side length of the unit cell and pore diameter, i.e. $l = 2.4589R^\circ$. Similarly, considering the equal pore-area, we find $l^{(1)} = 2.4589R^\circ$ and $t^{(1)} = 2.3543R^\circ$. In order to keep the self-consistency, we also employ the data of Al provided

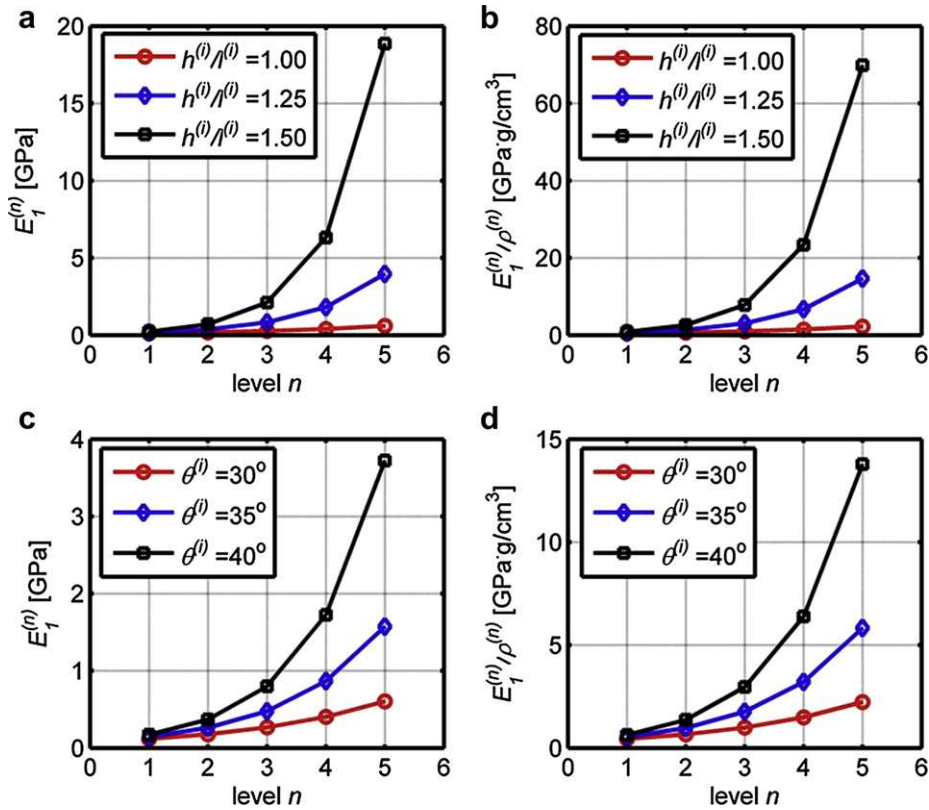


Fig. 7. (a) Influence of h/l on stiffness when $\theta = 30^\circ$; (b) Influence of h/l on stiffness-to-density ratio when $\theta = 30^\circ$; (c) Influence of θ on stiffness when $h/l = 1.0$; (d) Influence of θ on stiffness-to-density ratio when $h/l = 1.0$.

by Miller and Shenoy (2000); the bulk Young's modulus is $E^{(0)} = 89.392$ GPa, and surface Young's modulus on the [100] and [111] surface for plates are $E_s^{(0)} = -7.9146$ N/m and $E_s^{(0)} = 5.1811$ N/m, respectively. The results are reported in Fig. 6, in which the Young's moduli and bulk modulus of the honeycombs are normalized by those of the honeycombs without surface effect.

Fig. 6 shows, as the beam size increases, that the influence of the surface effect on the elastic constants decreases. Also, we find that generally our prediction is comparable with the result from the literature, even though our result shows a slightly greater influence; besides the different geometries, the thickness-to-length ratio $t^{(1)}/l^{(1)}$ is 0.93 under the condition of the porosity 0.2, that is to say, the shear effect should be taken into account.

6. Parametric analysis and discussion

Here, again, we consider Al as the constituent material and treat different hierarchical nano-honeycomb structures with hierarchical level number from one to five and identical relative densities (low relative density 0.1 is considered). We assume the size of the cell wall is very large compared with that of the first level, so, the surface effects at level i ($i > 1$) are negligible. The density of Al is 2.70 g/cm³; the surface elastic modulus on the [100] surface is $E_s^{(0)} = -7.9146$ N/m; the thickness of the cell walls at the first level is assumed to be $t^{(1)} = 5$ nm.

6.1. Linear-elastic deformation analysis

As we discussed in Section 3, the Young's moduli and shear modulus depend on the longitudinal Young's modulus, thus, $E_1^{(n)}$ is

only analyzed. We consider self-similar cases for n -level structures, i.e. the relative density $\rho^{(i+1)}/\rho^{(i)} = \sqrt[3]{0.1}$ and $h^{(i)}/l^{(i)} = h/l$ (or $\theta^{(i)} = \theta$). The analytic results of the longitudinal Young's modulus and the stiffness-to-density ratio are reported in Fig. 7. It shows that the longitudinal Young's modulus increases as h/l or θ increase; we can also see that as the level number n increases, they increase.

6.2. Buckling analysis

In this case, the parameters are the same as those described above. The analytic results of the buckling strength and strength-to-density ratio are reported in Fig. 8. Interestingly, it shows that increasing h/l or θ results in high strength and strength-to-density ratio and as the level number n increases, the strength and strength-to-density ratio reaches an optimal value in the three-level structure (Fig. 8a and b) or in the four-level structure for different parameters (Fig. 8c and d).

6.3. Discussion

Figs. 7 and 8 indicate that the mechanical behavior of the hierarchical honeycomb can be tuned by changing the geometrical configuration. Increasing h/l or θ , the Young's modulus, strength and their corresponding mechanical efficiency increase; and as the level number n increases, also, they increase. For the linear-elastic analysis, this is because the structural deformation decreases when h/l or θ increases, then, the Young's modulus increases. For the buckling analysis, it can be understood that increasing h/l or θ or level number n results in a higher structural stiffness but, as level

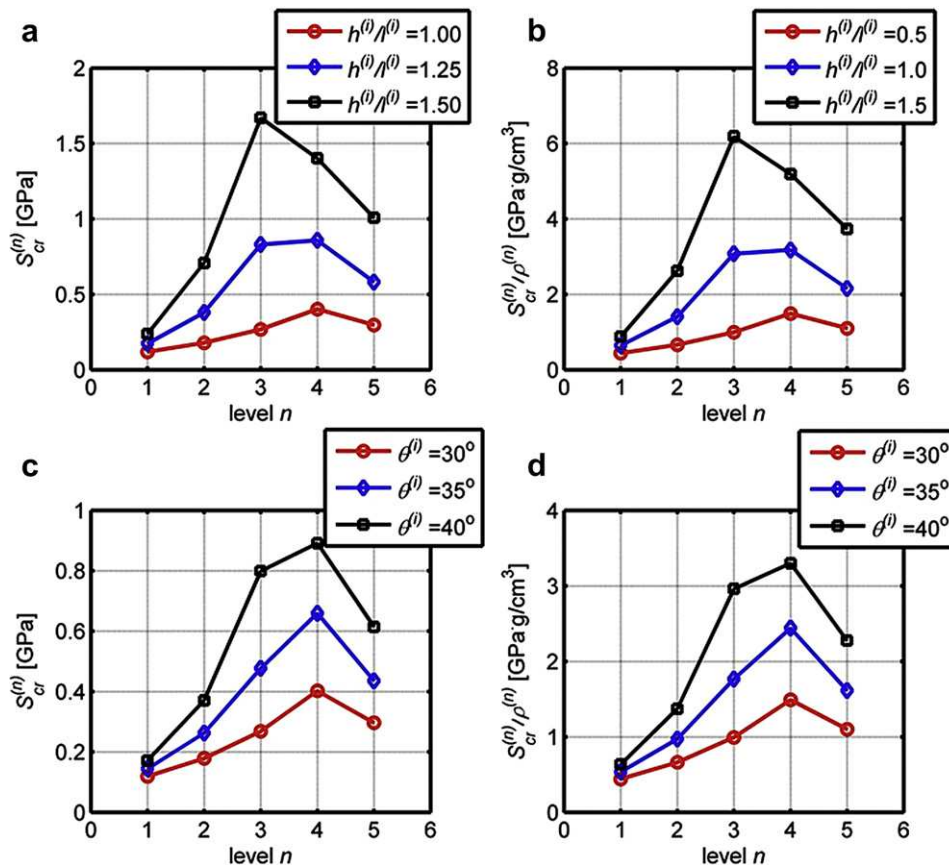


Fig. 8. (a) Influence of h/l on buckling strength when $\theta = 30^\circ$; (b) Influence of h/l on strength-to-density ratio when $\theta = 30^\circ$; (c) Influence of θ on buckling strength when $h/l = 1.0$; (d) Influence of θ on strength-to-density ratio when $h/l = 1.0$.

number n increases, the relative density at each hierarchical $\rho^{(i)}/\rho^{(0)}$ decreases, thus an optimal value emerges.

7. Conclusions

We have calculated the in-plane elastic properties (linear-elastic and buckling properties) of hierarchical nano-honeycombs. The surface effect modifies the classical results of a non-hierarchical honeycomb (or conventional honeycomb), which is considered to be the first level (or one-level structure); the predictions are compared with results from the literature, showing a good agreement. Addressing the hierarchical nano-honeycomb structures, we have performed parametric analyses, and revealed the influences of two key geometric parameters on the stiffness (or stiffness-to-density ratio) and strength (or strength-to-density ratio); the results show that increasing the two geometric parameters can produce increasing mechanical properties; in particular, an optimal strength or strength efficiency is obtained. The presented theory may have many interesting applications, e.g. for designing biomedical or energy-absorption nano materials.

Acknowledgments

The research related to these results has received funding from the European Research Council under the European Union's Seventh Framework Programme (FP7/2007–2013)/ERC Grant agreement nu [279985] (ERC StG Ideas to NMP on “Bio-inspired hierarchical super nanomaterials”).

References

- Ashby, M.F., 2010. *Materials Selection in Mechanical Design*, fourth ed. Butterworth-Heinemann, Burlington, US.
- Bezazi, A., Remillat, C., Innocenti, P., Scarpa, F., 2008. In-plane mechanical and thermal conductivity properties of a rectangular-hexagonal honeycomb structures. *Compos. Struct.* 84, 248–255.
- Budiansky, B., 1999. On the minimum weights of compression structures. *Int. J. Solids Struct.* 36, 3677–3708.
- Cammarata, R.C., 1994. Surface and interface stress effect in thin films. *Prog. Surf. Sci.* 46, 1–38.
- Chen, Q., Pugno, N., 2012a. Competition between in-plane buckling and bending collapses in nanohoneycombs. *Europhys. Lett.* 98, 16005.
- Chen, Q., Pugno, N., 2012b. In-plane elastic buckling of hierarchical honeycomb materials. *Eur. J. Mech. A Solid.* 34, 120–129.
- Chen, Q., Pugno, N., 2012c. Mechanics of hierarchical 3-D nanofoams. *Europhys. Lett.* 97, 26002.
- Duan, H., Wang, J., Karihaloo, B.L., Zhang, Z.P., 2006. Nanoporous materials can be made stiffer than non-porous counterparts by surface modification. *Acta Mater.* 54, 2983–2990.
- Duan, H., Wang, J., Karihaloo, B.L., 2009. Theory of elasticity at the nanoscale. *Adv. Appl. Mech.* 42, 1–68.
- George, J., Onodera, J., Miyata, T., 2008. Biodegradable honeycomb collagen scaffold for dermal tissue engineering. *J. Biomed. Mater. Res. A* 87, 1103–1111.
- Gibson, L.J., Ashby, M.F., 1997. *Cellular Solids: Structure and Properties*, second ed. Cambridge University Press, Cambridge.
- Gibson, L.J., Ashby, M.F., Schajer, G.S., Robertson, C.J., 1982. The mechanics of two-dimensional cellular materials. *Proc. R. Soc. Lond. A* 382, 25–42.
- Gurtin, M.E., Murdoch, A.I., 1975. A continuum theory of elastic material surface. *Arch. Rat. Mech. Anal.* 57, 291–323.
- Karam, G.N., Gibson, L.J., 1994. Biomimicking of animal quills and plant stems: natural cylindrical shells with foam cores. *Mater. Sci. Eng. C* 2, 113–132.
- Lakes, R., 1993. Materials with structural hierarchy. *Nature* 361, 511–515.
- Miller, R.E., Shenoy, V.B., 2000. Size-dependent elastic properties of nanosized structural elements. *Nanotechnology* 11, 139–147.
- Papka, S.D., Kyriakides, S., 1994. In-plane compressive response and crushing of honeycombs. *J. Mech. Phys. Solids* 42, 1499–1532.
- Pugno, N.M., Borgia, F., Carpinteri, A., 2008. Multiscale stochastic simulations for tensile testing of nanotube-based macroscopic cables. *Small* 4, 1044–1052.
- Pugno, N.M., 2006. Mimicking nacre with super-nanotubes for producing optimized super-composites. *Nanotechnology* 17, 5480–5484.
- Raabe, D., Romano, P., Sachs, C., Al-Sawalimih, A., Brokmeier, H.-G., Yi, S.-B., Servos, G., Hartwig, H.G., 2005. Discovery of a honeycomb structure in the twisted plywood patterns of fibrous biological nanocomposite tissue. *J. Cryst. Growth* 283, 1–7.
- Rhee, H., Horstemeyer, M.F., Ramsay, A., 2011. A study on the structure and mechanical behavior of the *Dasyatis novemcinctus* shell. *Mater. Sci. Eng. C* 31, 363–369.
- Roark, R.J., Young, W.C., 1975. *Formulas for Stress and Strain*, fifth ed. McGraw-Hill Book Co. Inc., New York.
- Seki, Y., Schneider, M.S., Meyers, M.A., 2005. Structure and mechanical behavior of a toucan beak. *Acta Mater.* 53, 5281–5296.
- Shankar, M.R., King, A.H., 2007. How surface stresses lead to size-dependent mechanics of tensile deformation in nanowires. *Appl. Phys. Lett.* 90, 141907.
- Shenoy, V.B., 2005. Atomistic calculations of elastic properties of metallic fcc crystal surfaces. *Phys. Rev. B* 71, 094104–094111.
- Timoshenko, S.P., Gere, J., 1961. *Theory of Elastic Stability*, second ed. McGraw-Hill Company, New York.
- Tolf, G., 1985. Saint-Venant bending of an orthotropic beam. *Compos. Struct.* 4, 1–14.
- Wadley, H.N.G., 2006. Multifunctional periodic cellular metals. *Phil. Trans. R. Soc. A* 364, 31–68.
- Wang, G.F., Feng, X.Q., 2009. Surface effects on buckling of nanowires under uniaxial compression. *Appl. Phys. Lett.* 94, 141913.
- Wang, J., Duan, H.L., Huang, Z.P., Karihaloo, B.L., 2006. A scaling law for properties of nano-structured materials. *Proc. R. Soc. A* 462, 1355–1363.
- Wang, D., Wang, Z., Liao, Q., 2009. Energy absorption diagrams of paper honeycomb sandwich structures package. *Technol. Sci.* 22, 63–67.
- Wang, D., 2009. Impact behavior and energy absorption of paper honeycomb sandwich panels. *Int. J. Impact Eng.* 36, 110–114.
- Warren, W.E., Kraynik, A.M., 1987. Foam mechanics: the linear elastic response of two-dimensional spatially periodic cellular materials. *Mech. Mater.* 6, 27–37.
- Wegst, U.G.K., Ashby, M.F., 2004. The mechanical efficiency of natural materials. *Philos. Mag.* 84, 2167–2181.
- Wong, E.W., Sheehan, P.E., Lieber, C.M., 1997. Nanobeam mechanics: elasticity, strength and toughness of nanorods and nanotubes. *Science* 277, 1972–1975.
- Zhang, J., Ashby, M.F., 1992. Buckling of honeycombs under in-plane biaxial stresses. *Int. J. Mech. Sci.* 34, 491–509.
- Zhang, K., Duan, H., Karihaloo, B.L., Wang, J., 2010. Hierarchical, multilayered cell walls reinforced by recycled silk cocoons enhance the structural integrity of honeybee combs. *Proc. Natl. Acad. Sci. U. S. A.* 107, 9502–9506.